THE PENNSYLVANIA STATE UNIVERSITY
SCHREYER HONORS COLLEGE

DEPARTMENT OF AEROSPACE ENGINEERING

NUMERICAL MODELING OF A 17.8-GHz MICROWAVE ELECTROTHERMAL THRUSTER

SWARNA SINHA
SPRING 2013

A thesis
submitted in partial fulfillment
of the requirements
for baccalaureate degrees
in Aerospace Engineering and Mathematics
with honors in Aerospace Engineering

Reviewed and approved* by the following:

Michael M. Micci
Professor of Aerospace Engineering
Thesis Supervisor

Sven G. Bilén
Associate Professor of Engineering Design, Electrical Engineering, and Aerospace Engineering
Thesis Supervisor

Dennis K. McLaughlin
Professor of Aerospace Engineering
Honors Adviser

Robert G. Melton
Professor of Aerospace Engineering
Director of Undergraduate Studies

* Signatures are on file in the Schreyer Honors College.

ABSTRACT

This research is focused on the development of a CubeSat-scale Microwave Electrothermal Thruster (MET). The MET is an in-space propulsion device that utilizes high electric field intensity generated by a microwave antenna to ignite and sustain free-floating plasma within a cylindrical, electromagnetic resonant cavity. The propellant gas is heated and then expanded through a nozzle. Previous iterations of MET frequencies of 2.45 GHz, 7.5 GHz, 8 GHz, 14.5 GHz, and 30 GHz have all examined the performance of this technology. Higher frequency leads to smaller thruster size, lower power requirements, and a lighter overall propulsion system, albeit at lower thrust levels. This thesis discusses the design of a 17.8-GHz thruster cavity based on numerical simulations of electric field intensity within the thruster's resonant cavity using COMSOL Multiphysics.

TABLE OF CONTENTS

LIST OF FIGURES

ACKNOWLEDGEMENTS

I would like to thank Dr. Micci for offering me valuable advice in understanding concepts and solution methods, which allowed me to learn faster than I would have otherwise. I would also like to thank Dr. Bilén for his constant feedback and the many helpful resources he pointed out to me. With electromagnetic theory in particular, he helped me understand the critical concepts I had difficulty with early on.

With using COMSOL Multiphysics, I thank Pierre-Yves Taunay in addition to Dr. Bilén and Dr. Micci for guidance in using the software. Many students in the lab also deserve credit for providing me useful feedback on my work, on top of keeping the environment fun and interesting.

I thank my family for their tremendous support and encouragement. My sister and brother-in-law have always been eager to lend their support and are constant sources of inspiration. Finally, I would like to thank my parents for being my best teachers in basic principles of learning, hard work, and dedication, without which I would not have come this far.

Chapter 1

Introduction

The Microwave Electrothermal Thruster (MET) uses the electrothermal method to generate thrust by injecting microwave energy in a cylindrical thruster cavity. Propellant is inserted tangentially at a sufficiently low pressure to allow breakdown of the gas into plasma. The heated plasma is then expanded out of a nozzle, generating thrust on the order of millinewtons.

Potential applications of the MET include fine attitude control on satellites, and maneuvers and formation flight on small to medium sized satellites. Cube Satellites, or CubeSats, are viable users of this technology. Since they have low mass and limited space, they require a small propulsion system that uses minimal fuel mass and provides adequate thrust. CubeSats are also developed with off-the-shelf components and have significant technological capability due to miniaturization of space components. These facts indicate that costs of CubeSats are significantly lower than those of larger satellites. A small propulsion device such as the MET can add flexibility to CubeSat missions. The added capability to change orbits and orientation can add precision to any collection of science data, for example. Orbit lifetime can also increase, since the thrusters can occasionally counteract perturbation effects due to atmospheric drag [1].

The MET's performance depends on the intensity of the electric field produced near the nozzle since the electric field initiates and sustains plasma formation. Previous designs of larger METs, including the 2.45-GHz, 7.5-GHz, 8-GHz, and 14.5-GHz models have used various methods to create the optimal design. After empty MET cavity designs were found to allow plasma formation near the antenna, a dielectric insert was introduced to confine the plasma towards the nozzle end. For the 30-GHz MET design, which was very small in size, difficulties

arose in achieving plasma ignition due to the small chamber size tolerances that allowed functionality [2, 3, 4].

The objective of this thesis is to dimension and numerically analyze electric field intensities of somewhat larger MET design with a resonant frequency of 17.8-GHz. This MET is sized to meet CubeSat mass, power, and volume limitations. The theory of the MET's operation are discussed, followed by numerical electromagnetic simulations of electric fields within the cavity for different antenna configurations.

Introduction to CubeSats

CubeSat programs first appeared in 1999 out of collaboration between California Polytechnic State University and Stanford University. The program was geared towards making an affordable satellite program for students. Applications include Earth imaging, communications, and science experiments. Although the purpose of CubeSats was initially related to students, there has been a growing interest among government organizations and private companies [5]. However, objectives such as orbit change, formation flight, fine attitude control, and deorbiting all require an onboard propulsion system that is adequately small, lightweight, and powerful. Without a propulsion capability, CubeSat operations are very limited.

A single unit, or 1U, CubeSat is a cube measuring 10 cm along each edge and weighing about 1.33 kg. CubeSats may consist of multiple units as well. A 3U CubeSat weighs about 3 kg and consists of 3 cubes with edges measuring 10 cm long. For the purposes of this report, more focus is given to the 3U configuration since available power goes up to 10 W, as opposed to 1.6 W for a 1U CubeSat [6]. An electric propulsion system such as the MET requires power in addition to the power intake of other systems onboard. Including losses in power transmission,

the delivered power to the propulsion system will also be significantly under the available power. For these reasons, the 3U CubeSat's available power is preferable.

Safety is another critical factor in propulsion system design. Parts must be highly reliable. All sealing components such as valves and O-rings must be redundant up to even triple redundancy, if possible. The propulsion system should preferably use stable fuels that will take up minimal space without compromising performance. Costs per unit should also be minimal in a range of $100k – 250k [5].

Performance of the system should deliver enough delta-V for orbit raising and plane change at various orbital altitudes. Plane changes require around 131.0 – 135.4 (m/s)/deg for a CubeSat at Earth orbital altitudes from 250 – 750 km. An altitude change for 1 km requires 0.58 m/s of delta-V at 250 km, decreasing to 0.52 m/s at 750 km.

Performance is also dependent on the dry mass fraction, which is defined as empty spacecraft mass divided by the fueled spacecraft mass. The relationship between this fraction and delta-V is given by

$$\Delta v = g I_{\mathrm{sp}} \ln\left(M_i / \left(M_i - M_p\right)\right), \tag{1.1}$$

where I_{sp} is the specific impulse, g is gravitational acceleration, M_i is initial mass, and M_p is propellant mass. For different values of I_{sp}, a graphical representation of Eq. 1.1 is shown in Figure 1-1. Lower dry mass fraction and higher I_{sp} lead to higher delta-V capabilities [5].

I_{sp} depends on the propellant's composition. When considering the use of a monopropellant system in comparison with a bipropellant system, the bipropellant system typically has greater I_{sp}. However, the mass of a bipropellant system is much greater due to plumbing and storage of fuel and oxidizer. In general, it is more complex and expensive than a monopropellant system, which still has enough I_{sp} while promising reliability, part availability, and more propellant availability. Therefore, monopropellant systems have a significant advantage. On the other hand, catalyst beds in monopropellant systems have suffered from

erosion, affecting the longevity of the overall system. Fortunately, in the case of electrothermal thrusters, catalyst beds are not required [6].

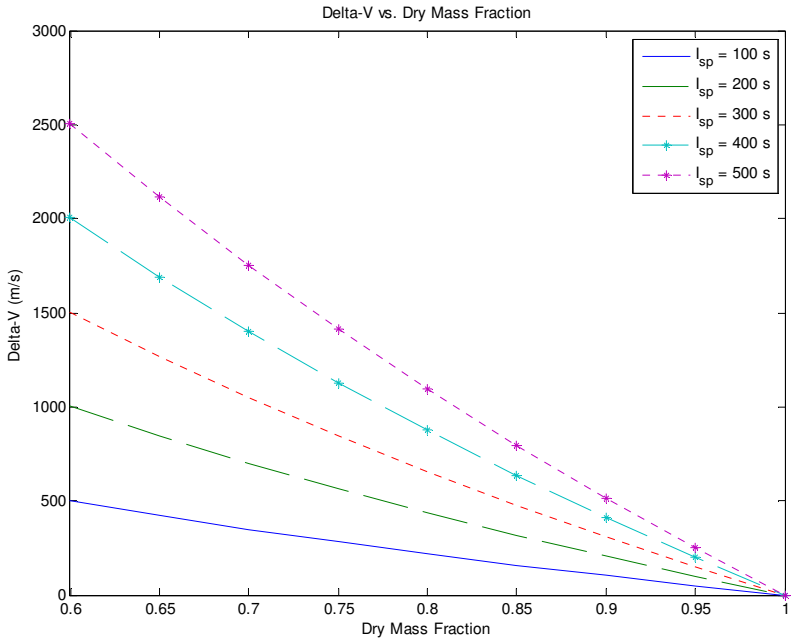

Figure 1-1. Delta-V vs. Dry Mass Fraction

A wide range of chemical and electric propulsion systems that may fulfill CubeSat requirements exist. Electric propulsion systems are of particular interest because they use less propellant compared with chemical systems. Less propellant leads to less space necessary for storage within the CubeSat, which already has limited space.

Electric propulsion systems fall into three separate categories: electrostatic, electrothermal, and electromagnetic. Electrostatic propulsion creates thrust by accelerating discrete charged particles, usually atoms, with electrostatic forces. Electron bombardment charges the atoms. Electromagnetic propulsion uses electromagnetic and pressure forces to accelerate a stream of electrically conducting fluid. This method is most effective in pulsed operations.

Finally, electrothermal propulsion consists of applying electrical heating to a fluid propellant. Electromagnetic fields can add heat by ionizing the propellant gas to create plasma.

While some electrostatic and electromagnetic thrusters require less propellant, their applications are limited. A propellantless electromagnetic propulsion system, for example, must use high current electromagnetic coils in order to generate enough force. The coils operate at high temperatures that may affect the functionality of other scientific instruments onboard. However, the temperatures are difficult to regulate within confined regions of the CubeSat's volume, which is already small. Ion propulsion systems, while lending high I_{sp} values, are difficult to miniaturize and require more power than a 3U CubeSat could deliver without deployable solar arrays. Such systems that contain electrodes also suffer from long-term erosion, compromising the system's lifespan. Micro-Pulsed Plasma Thrusters have shown some promise but also are challenging to miniaturize. In addition, their delta-V is small [6].

The main challenges in developing a CubeSat propulsion system involve minimizing the size, using a safe and storable propellant, using reliable and redundant parts that remain relatively intact over time, maintaining functionality with a power input under 10 W, and retaining performance in terms of delta-V and I_{sp}.

Chapter 2

MET Theory

This chapter describes the operation of the MET and presents the theoretical equations and boundary conditions of the TM^{Z}_{011} resonant cavity mode. The theory is implemented to size the cavity with a resonant frequency 17.8 GHz. Microwave breakdown is explained with a focus on the use of ammonia as a green propellant, which is a safe and environmentally friendly alternative to commonly used propellants in spacecraft thrusters.

Basic Operational Principles of the MET

The MET's resonant cavity is designed as a cylinder that concentrates electric energy density at the endplates along the cavity's axis. Figure 2-1 shows a schematic of the MET. The antenna feeds through the lower endplate and inputs microwave power into the cavity. A dielectric plate placed at the mid-plane of the cavity is used to allow different pressures on either side. The antenna section is maintained at atmospheric pressure while the nozzle section is evacuated. This prevents breakdown from occurring at the antenna.

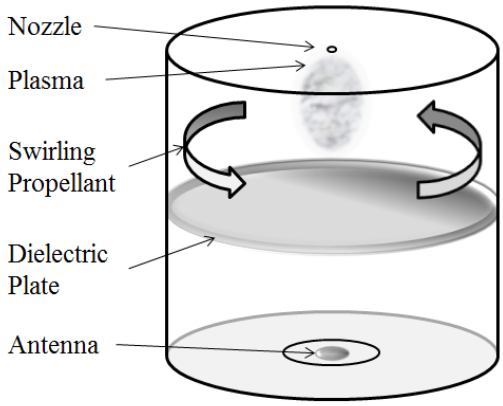

Figure 2-1. MET Schematic

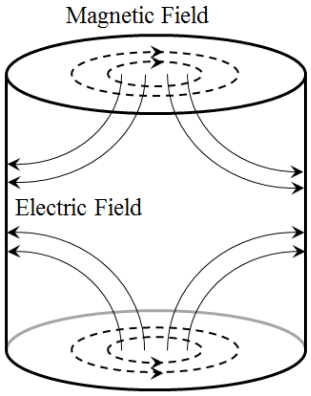

Figure 2-2. MET TM^{z}_{011} Mode Diagram

Propellant is injected tangentially through two ports located close to the nozzle and directly across from each other. With this method, the propellant swirls and promotes axial stability of the discharge. Electric field intensity must be optimized at the nozzle end to produce axial, free-floating plasma. The transverse magnetic TM^{z}_{011} mode, shown in Figure 2-2, is optimal for this purpose since electric field strength is highest at the endplates. Selection of the proper height-to-radius ratio of the cavity increases electric field strength at the endplates relative to that of the cavity's mid-plane [7].

TM^{z}_{011} Resonant Cavity Field Theory

Electromagnetic field theory of the MET is derived using Maxwell's Equations. A set of second-order differential equations with wave solutions are solved using vector potentials in cylindrical coordinates with the following boundary conditions:

$$E_{\phi}(0 \leq \rho \leq a, 0 \leq \phi \leq 2\pi, z = 0, h) = 0 \tag{2.1}$$

$$E_{z}(\rho = 0, a, 0 \leq \phi \leq 2\pi, 0 \leq z \leq h) = 0 \tag{2.2}$$

For the TM^{z}_{011} resonant mode, Eqs. (2.3) through (2.8) include the electrical and magnetic field components for a cylindrical cavity that is a perfect conductor and filled with a homogeneous, lossless, and source-free medium.

$$E_\rho = j\frac{B_{011}}{\omega\mu\varepsilon}\frac{\pi\chi_{01}}{ah}J_0'\left(\frac{\chi_{01}}{a}\rho\right)\sin\left(\frac{\pi z}{h}\right) \tag{2.3}$$

$$E_\phi = 0 \tag{2.4}$$

$$E_z = -j\frac{B_{011}}{\omega\mu\varepsilon}\left(\frac{\chi_{01}}{a}\right)^2 J_0'\left(\frac{\chi_{01}}{a}\rho\right)\cos\left(\frac{\pi z}{h}\right) \tag{2.5}$$

$$H_\rho = 0 \tag{2.6}$$

$$H_\phi = -\frac{B_{011}}{\mu}\frac{\chi_{01}}{a}J_0'\left(\frac{\chi_{01}}{a}\rho\right)\cos\left(\frac{\pi z}{h}\right) \tag{2.7}$$

$$H_z = 0 \tag{2.8}$$

Resonant frequency within the chamber is related to chamber radius and height by

$$(f_{\text{res}})^{\text{TM}^z}_{011} = 17.8\text{ GHz} = \frac{1}{2\pi\sqrt{\mu\varepsilon}}\sqrt{\left(\frac{\chi_{01}}{a}\right)^2 + \left(\frac{\pi}{h}\right)^2} \tag{2.9}$$

Varying the height-to-radius ratio, h/a, alters the electric field strength at the endplates relative to that of the midplane [8]. This ratio is given by

$$\left|\frac{E_z|_{\rho=0,z=h}}{E_\rho|_{\rho=a,z=h/2}}\right| = \left[\frac{\chi_{01}}{\pi}\frac{J_0(0)}{J_1(\chi_{01})}\right]\left(\frac{h}{a}\right) = 1.472\left(\frac{h}{a}\right) \tag{2.10}$$

where $\chi_{01} = 2.4049$ [9].

Higher h/a increases the proportion of electric field strength near the nozzle, which is crucial for ionizing the propellant gas and sustaining plasma formation. Designs for the 14.5-GHz and 30-GHz METs set $h/a = 3.5$ [2, 3]. However, designs incorporating a dielectric plate at the midplane, such as the 2.45-GHz MET design, had a lower $h/a \approx 3$. Fig. 3 shows the variation of resonant frequency with respect to h/a with three different values for radius. Altering the radius by as little as a millimeter drastically alters the resonant frequency. MATLAB code for

generating Fig. 3 is located in the Appendix. For smaller MET designs, these changes have larger impacts than in larger designs, such as the 2.45-GHz and 7.5-GHz METs [4].

The addition of a dielectric plate at the mid-plane adds further complexity to determining cavity dimensions. Resonant wavenumber is defined by

$$\beta_{\text{res}}^2 = \omega_{\text{res}}^2 \mu\varepsilon = \beta_\rho^2 + \beta_z^2 \tag{2.11}$$

The field equations with the dielectric plate included are the following three equations [2]:

$$\frac{\beta_{z,d}}{\varepsilon_d}\tan(\beta_{z,d}t) = \frac{\beta_{z,g}}{\varepsilon_g}\tan\left(\beta_{z,g}(t-h)\right) \tag{2.12}$$

$$\beta_{z,d} = \sqrt{\beta_{d,\text{res}} - \beta_r^2} = \sqrt{\omega_{\text{res}}^2 \mu_d \varepsilon_d - \left(\frac{\chi_{mn}}{a}\right)^2} \tag{2.13}$$

$$\beta_{z,g} = \sqrt{\beta_{g,\text{res}} - \beta_r^2} = \sqrt{\omega_{\text{res}}^2 \mu_g \varepsilon_g - \left(\frac{\chi_{mn}}{a}\right)^2} \tag{2.14}$$

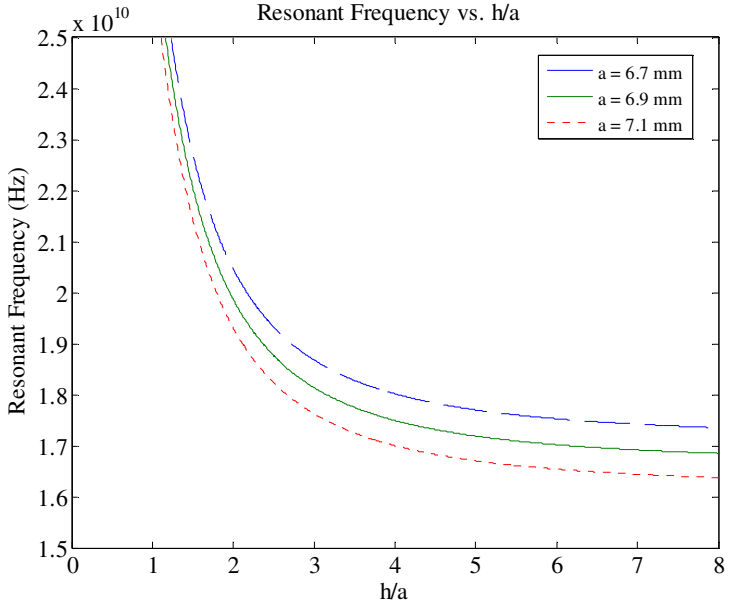

Figure 2-3. Resonant Frequency vs. *h/a*

The presence of the plate, which is made of fused quartz that has $\varepsilon_d = 4.2\varepsilon_0$, lowers the resonant frequency of the cavity. Therefore, the overall height of the cavity must be reduced accordingly. The value of ε_g is set to be equivalent to ε_0.

Since high dielectric plate thicknesses, t, lower the resonant frequency by a large amount, a minimum $t = 1/16"$ (1.5875 mm) was selected based on availability and strength requirements, which include the plate's ability to endure stress from pressure of at least 1 atm (1.01×10^5 Pa). With this value of t and implementation of Eqs. (2.12) through (2.14), the cavity radius is 6.8 mm. The optimal height of 21.1 mm was determined using COMSOL Multiphysics. The resulting $h/a \approx 3.1$.

Breakdown Ionization

The MET generates thrust by using a plasma discharge to heat a propellant gas. In the resonant cavity, applying a strong electric field to the gas forms a free-floating discharge. The transformation of a non-conducting material into a conductor via application of a sufficiently strong field, called electric breakdown, strips electrons from neutral particles. The discharge will ignite and sustain itself as long as the field is applied for a sufficient period of time.

Once a few primary electrons in the gas gain energy from the primary field, they collide with the surrounding neutral particles and ionize them, assuming they have sufficient energy. New free electrons are released. Although the energy of the initial and new free electrons temporarily drops after the collision, the electric field gives them more energy and accelerates them again, causing the chain reaction to continue. Whether or not the chain reaction sustains itself depends on losses in the system. For instance, vibrational and rotational modes in the atoms and molecules could absorb extra energy within the system. Exciting electron energy states within

the atoms and molecules also causes energy losses. For these reasons, selecting a lighter and less complex molecular structure is best for the MET's performance.

Electron losses may also end the chain reaction. Electrons can diffuse and adhere to the cavity walls instead of constantly colliding with molecules to free more electrons. Recombination of electrons and ionized molecules is another factor. However, recombination is not a significant loss factor in general, depending on the density of the gas. A discharge can be ignited and sustained as long as the rate of ionization just barely exceeds the rate of electron loss. This threshold depends on electric field strength, frequency, and gas pressure. The breakdown of gases in microwave fields occurs most easily at pressures of 1 – 10 Torr (0.13 – 1.33 kPa) [4].

Green Propellant

Environmental impacts of current space propulsion systems have signified a need for alternative propellants that reduce mission costs and risks, especially with anticipated increases in the number of spacecraft launches. These impacts may be ground-based, atmospheric, space-based, or biological impacts. Groundwater contamination due to mishandling of propellants leads to ground-based impacts. Propellant exhaust and subsequent air pollution affect the atmosphere. Space-based impacts relate to debris and spacecraft effects of propellant use. Finally, biological impacts concern the toxicity and corrosiveness of propellants [10]. While no propellant can completely eliminate any of these impacts, the objective is to minimize their effects as much as possible. A "green propellant" abides by this goal.

Conventional liquid propellants used in space thrusters include hydrazine and bipropellant formulations using liquid oxygen (LOX). Hydrazine is highly toxic, carcinogenic, and thus expensive to handle. It is also naturally unstable, which heightens the risk of ruptures and explosions in outer space. LOX requires bulky tanks, feedlines, and valves, which are not

optimal for spacecraft use either [10]. A more ideal propellant would be easily storable, relatively nontoxic, inexpensive to produce and handle, and stable.

The MET requires a lightweight propellant in order for breakdown to occur, since lighter molecules are easier to accelerate. Moreover, the compound should not be too complicated, as vibrational and rotational modes add further complications in electron excitation during the breakdown process. Currently, ammonia is a potential candidate, with the following chemical equilibrium equations:

$$NH_3 \rightleftharpoons \tfrac{1}{2}N_2 + \tfrac{3}{2}H_2 \tag{2.15}$$

$$N_2 \rightleftharpoons 2N \tag{2.16}$$

$$H_2 \rightleftharpoons 2H \tag{2.17}$$

Chemical equilibrium is assumed within the MET chamber, even though ammonia dissociation occurs slowly. At higher temperatures, reaction rates increase. Ammonia dissociates completely into H_2 and N_2 over a temperature range of 1000 – 2200 K. However, non-negligible amounts of H appear at 2200 K. At 4500 K, non-negligible amounts of N also appear [4].

Microwave breakdown of ammonia may be affected by the presence of individual or diatomic nitrogen and hydrogen molecules. Fortunately, ammonia has a very high electron attachment coefficient and low ionization potential, meaning that it is very effective in attaching electrons and that it is ionized more easily. Therefore, effects of N, H, N_2, and H_2 on the breakdown field will be very small. For pressures ranging from 1 – 10 Torr (0.13 – 1.33 kPa), the breakdown electric field of pure ammonia ranges is under 1×10^5 V/m. The effects of adding dry nitrogen up to 50% concentration to pure ammonia are not significant [11].

Chapter 3

Electromagnetic Modeling

COMSOL Multiphysics was used to generate a numerical simulation of electric field intensity throughout the cavity [12]. The cavity was divided into three subdomains. The first subdomain includes the air-filled cavity, which has a relative permittivity of 1. The second subdomain is the dielectric plate placed at the midpoint along the cavity's *z*-axis. The material is fused quartz and has a relative permittivity of 4.2. Finally, the third subdomain is the coaxial Teflon material around the antenna. This material has a relative permittivity of 2.0.

All walls and surfaces of the antenna were modeled as perfect electric conductors. The interfaces between the subdomains were modeled as continuous so that solutions of the wave equations were continuous throughout the full geometry. The port at the base of the Teflon material was set as a coaxial port having an input power of 1 W. A free tetrahedral mesh was generated containing nearly 35,000 elements. A high number of elements is vital for providing a clear numerical solution that is free of sharp discontinuities. However, the number was also low enough for a reasonable computation time.

The following COMSOL simulations analyze the effects of different antenna shapes and sizes on electric field distribution. The ideal result is to have a stronger electric field near the nozzle end. Each simulation performs a parametric sweep of resonant frequency values ranging from 17.725 GHz to 17.875 GHz. Graphs plotting the maximum electric field norm in the domain of the cavity between the nozzle end and dielectric plate versus frequency are also presented and discussed. Most simulations are not expected to peak exactly at 17.8 GHz. The microwave source is being specified to a tunable frequency range of ±0.075 GHz about this target value, allowing some tuning flexibility.

Cavity with Varying Antenna

Selection of the proper antenna size depends on the electric field intensity each option can produce. The available options include antennas with SMA, SSMA, and 2.4-mm connectors. Figure 3-1 shows the change in resonant frequency with different antenna sizes. As the antenna size decreases, the peak electric field intensity increases and the resonant frequency decreases. The 2.4-mm antenna produces a maximum electric field magnitude of about 2.4×10^6 V/m. However, even if more energy is concentrated at the resonant frequency using the 2.4-mm antenna, the range of frequencies over which the cavity is resonant is much smaller.

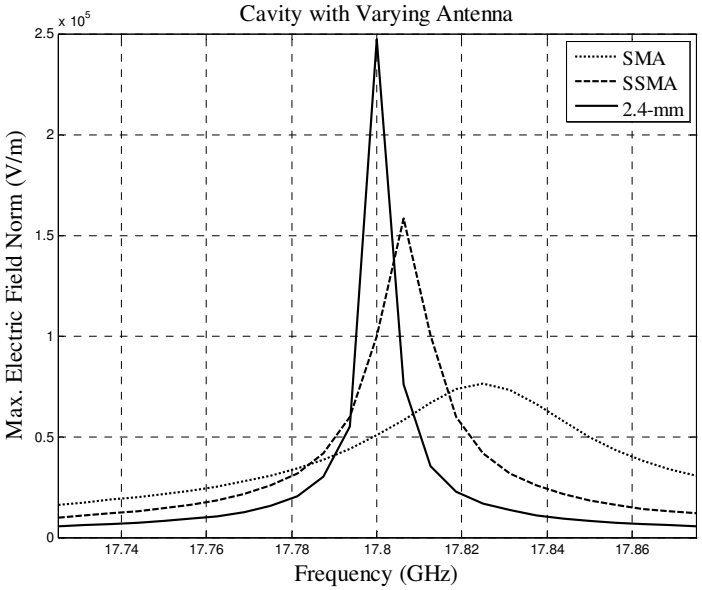

Figure 3-1. Cavity with SMA, SSMA, and 2.4-mm Antenna

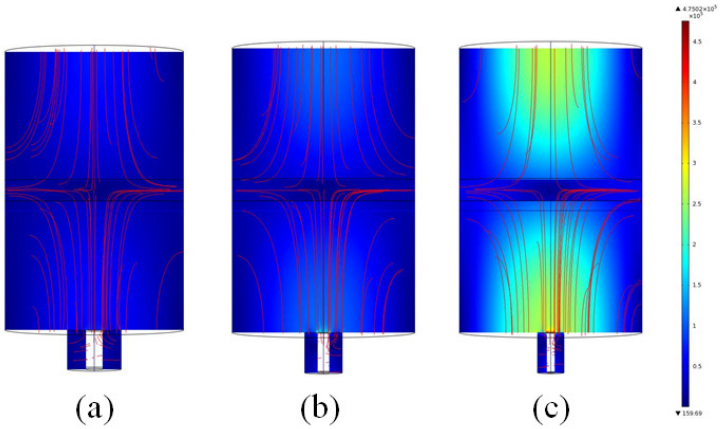

Figure 3-2. Electric Field Intensity Distribution for (a) SMA (b) SSMA and (c) 2.4-mm Antenna

As can be seen in Figure 3-2, the smaller the antenna, the more the electric field concentrates towards the endplates. For plasma ignition near the nozzle end, this result is best. The SSMA and SMA antennas perform much less effectively for this cavity geometry. To compare performances between the 2.4-mm antenna and SSMA antenna, antenna shape is varied in the following sections.

Cavity with 2.4-mm Antenna and Varying Antenna Shape

All antenna shapes initially had flat edges and were set flush with the inner cavity surface. Three additional configurations are simulated. The first has a hemispherically rounded antenna tip, the second has a flat tip that protrudes 0.5 mm into the cavity, and the third has the same rounded tip that protrudes 0.5 mm into the cavity.

Figure 3-3 displays the variation in resonant frequency. The rounded tips both widen the range of resonant frequencies for the cavity. However, the flat tips have higher peak electric field

strength. As the antenna protrudes further into the cavity, the resonant frequency decreases and the electric field intensity drops.

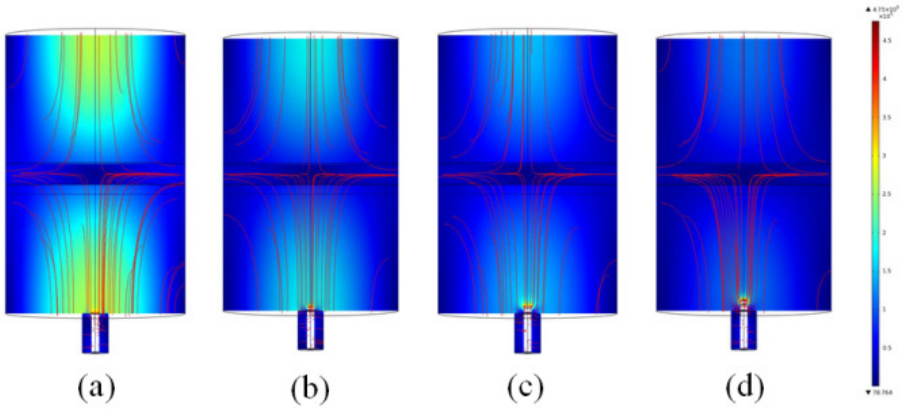

Figure 3-3. Electric Field Intensity Distribution of 2.4-mm Antenna for (a) flat (b) rounded and (c) +0.5-mm flat and (d) +0.5-mm rounded shapes

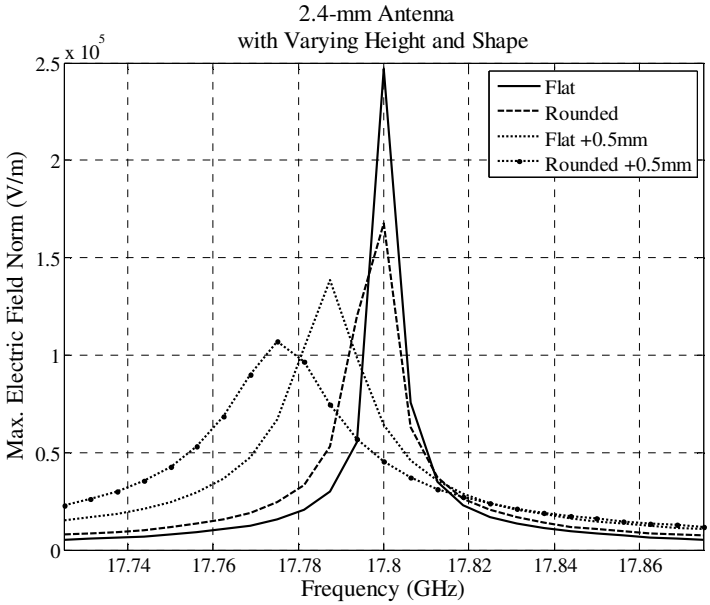

Figure 3-4. Varying Antenna Shape for 2.4-mm Antenna

COMSOL simulation results are shown in Figure 3-4 for the different antenna shapes. The electric field values shown reflect the maximum electric field norm only in the region near the nozzle end behind the dielectric plate. The behavior described in Figure 3-3 is visible with the diminishing field strength for antenna shapes that protrude into the cavity.

Cavity with SSMA Antenna and Varying Antenna Shape

The same variations in antenna shape used for the 2.4-mm simulations are implemented in the SSMA antenna model. The COMSOL results in Figure 3-5 are scaled for range of electric field strengths from 0 to 1.6×10^{6} V/m, which is the highest electric field strength produced by SSMA antenna model.

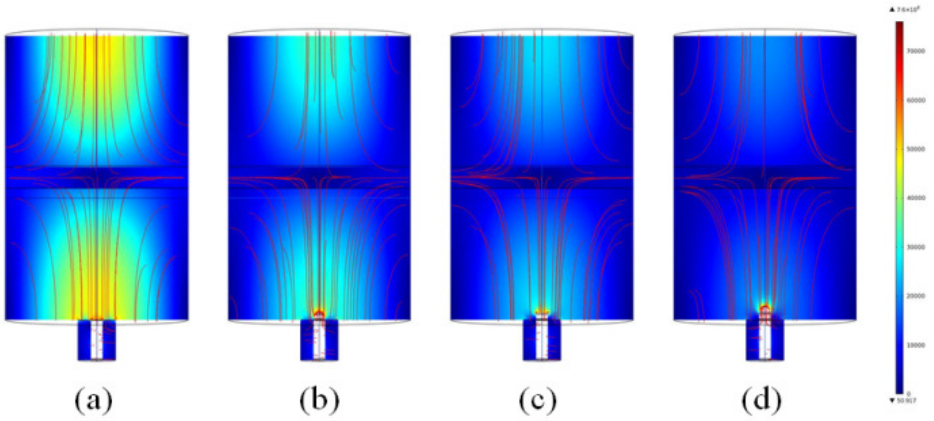

Figure 3-5. Electric Field Intensity Distribution of SSMA Antenna for (a) flat (b) rounded (c) +0.5-mm flat and (d) +0.5-mm rounded shapes

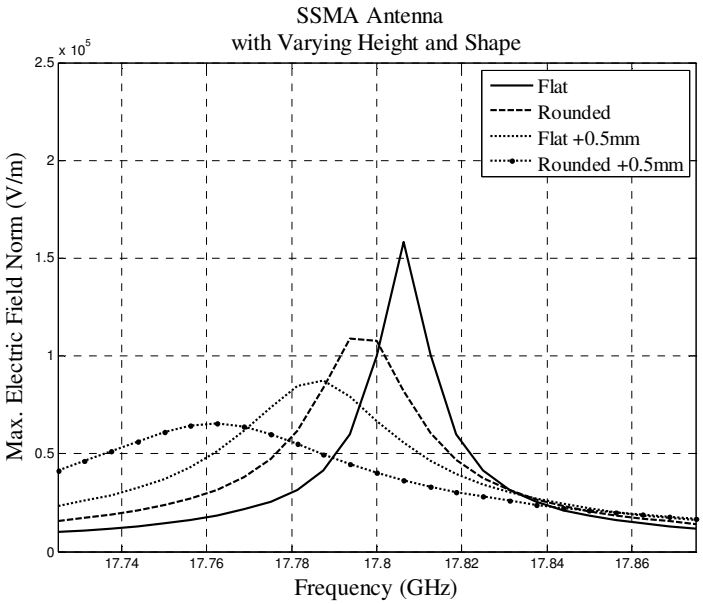

Figure 3-6. Varying Antenna Shape for SSMA Antenna

Electric field strength and resonant frequency both decrease with increasing antenna protrusion into the cavity. In Figure 3-6, the range of resonant frequencies that can sustain the highest possible electric field is wider for all antenna shapes aside from the flat case.

Chapter 4

Summary, Conclusions, and Future Work

The CubeSat-scale MET cavity has been designed for a resonant frequency of 17.8 GHz. METs are advantageous since they do not contain electrodes or catalyst beds that degrade over time. Since I_{sp} is higher than in chemical propulsion, less propellant is also needed to acquire adequate delta-V.

The cylindrical cavity was sized based on electromagnetic field theory solutions to obtain the TM^{Z}_{011} mode. The insertion of a dielectric plate made of fused quartz at the cavity's mid-plane altered resonant cavity dimensions, decreasing the overall height. COMSOL Multiphysics simulations were used to further optimize the cavity to a radius of 6.8 mm and height of 21.1 mm.

Simulation results showed that the 2.4-mm antenna yielded the strongest electric field at 2.4×10^5 V/m. The chamber dimensions were optimized to this antenna. Flat and rounded antenna tips produced stronger electric fields than antenna tips protruding further into the cavity. While the rounded tip has a weaker electric field than the flat tip, it allows the cavity to resonate at wider range of frequencies.

Microwave breakdown of a green propellant such as ammonia may occur using an electric field under 1×10^5 V/m. This study has defined optimal cavity dimensions and shown potential for generating enough electric field intensity for plasma ignition at 1 W. Given that the simulations were performed with an input power of 1 W and that a 3U CubeSat can deliver up to 10 W of power, the electric field can be increased further. Losses in power transmission can be verified to give an accurate estimate of delivered power in future work.

Since this study is mainly focused on electromagnetic fields, future COMSOL simulations should work with fluid flow to gain insight on pressure and temperature conditions within the cavity. Design of a physical thruster can proceed since the geometry has been

optimized to maximize electric field intensity. With realistic testing and results, simulated and experimental results can be compared and verified.

Appendix

MATLAB Scripts

```
% ------------------------------------------------------------
% Resonant Frequency vs. h/a
% ------------------------------------------------------------
% This script computes and plots resonant frequency as a function of
% cavity height-to-radius ratio using three different radii.
% ------------------------------------------------------------

clear all;

% Cavity radii
a1 = 6.9e-3;
a2 = 6.7e-3;
a3 = 7.1e-3;

% Constants
eg = 8.854e-12;
mu = 1.25664e-6;
x01 = 2.4049;

% Height-to-radius ratio, h/a
ratio = linspace(0,8,1000);

% Resonant frequency for the different cavity radii
f_res1 = (1/a1)*((x01^2+(pi./ratio).^2).^0.5)/(2*pi*(eg*mu)^0.5);
f_res2 = (1/a2)*((x01^2+(pi./ratio).^2).^0.5)/(2*pi*(eg*mu)^0.5);
f_res3 = (1/a3)*((x01^2+(pi./ratio).^2).^0.5)/(2*pi*(eg*mu)^0.5);

figure(1)
plot(ratio,f_res2,'--',ratio,f_res1,ratio,f_res3,':')
axis([0 8 1.5e10 2.5e10])
xlabel('h/a')
ylabel('Resonant Frequency (Hz)')
legend('a = 6.7 mm','a = 6.9 mm','a = 7.1 mm')
title('Resonant Frequency vs. h/a for Different Values of a')
% ------------------------------------------------------------
```

REFERENCES

[1] Marcuccio, S., Pergola, P., and Ruggiero, A. "Electric Propulsion Options for CubeSats." *62nd Astronautical Congress*, 2011.

[2] Adusumilli, R. P., "Performance Evaluation and Optimization of High Power 14.5-GHz Minature Microwave Electrothermal Thruster," M.S. Thesis, Dept. of Aerospace Engineering, Penn. State Univ., University Park, PA, 2011.

[3] Capalungan, E. C., "Design and Development of a 30-GHz Microwave Electrothermal Thruster," M.S. Thesis, Dept. of Aerospace Engineering, Penn. State Univ., University Park, PA, 2011.

[4] Clemens, D. E., "Performance Evaluation of the Microwave Electrothermal Thruster Using Nitrogen, Simulated Hydrazine, and Ammonia," Ph.D. Dissertation, Dept. of Aerospace Engineering, Penn. State. Univ., University Park, PA, 2008.

[5] Biddy, C. L. "Development of a High Performance Micropropulsion System for CubeSats," M.S. Thesis, Mechanical Engineering Department, California Polytechnic State University, San Luis Obispo, CA, 2009.

[6] Mueller, J., Hofer, R., Ziemer, J. "Survey of Propulsion Technologies Applicable to CubeSats." Jet Propulsion Laboratory, Pasadena, CA.

[7] Micci, M. M., Bilén, S.G., and Clemens, D.E. "History and Current Status of the Microwave Electrothermal Thruster," *2nd European Conference for Aerospace Sciences (EUCASS)*, 2007.

[8] Balanis, C. A., *Advanced Engineering Electromagnetics*, John Wiley & Sons, Inc., Hoboken, 1989.

[9] Gao, E., and Bilén, S.G. "COMSOL Multiphysics Modeling of a 20-W Microwave Electrothermal Thruster," *COMSOL Conference,* Boston, 2008.

[10] Desain, J. D. "Green Propulsion: Trends and Perspectives." *Crosslink Magazine*, The Aerospace Corporation, El Segundo, CA, 2011.

[11] Gilardini, A. L., McCarthy, J. J., Gordon, E. I., Buchsbaum, S. J. "Microwave Gaseous Discharges," Research Laboratory of Electronics (RLE) at the Massachusetts Institute of Technology (MIT), 1995.

[12] COMSOL Multiphysics, Ver. 4.2, COMSOL, Inc., Burlington, MA, 2011.

ACADEMIC VITA

Swarna Sinha
171 Meadow Lark Lane, Boalsburg, PA, 16827
swarnasinha@gmail.com

Education

B.S., Aerospace Engineering, 2013, Pennsylvania State University, University Park, PA
B.S., Mathematics, 2013, Pennsylvania State University, University Park, PA

Honors and Awards

- Whole World Scholarship, 2010

Association Memberships/Activities

- American Institute of Aeronautics and Astronautics (AIAA), Student Member
- Sigma Gamma Tau Honors Society

Professional Experience

- Undergraduate Honors Thesis, University Park, PA (Spring 2012 – Spring 2013)
  - Development of CubeSat-scale Microwave Electrothermal Thruster (MET) with Dr. Michael M. Micci and Dr. Sven G. Bilén
- NASA Ames Research Center, Moffett Field, CA (Summer 2012)
  - NASA Ames Academy for Space Exploration 2012
  - Characterized star tracker emulator on LADEE spacecraft test bed
  - Designed power system for group project SALEE
- MIT Space Systems Laboratory, Cambridge, MA (Summer 2011)
  - Designed sensor circuit and contributed to report and presentation of TERSat satellite's preliminary design review
  - Created educational materials and game players for Zero Robotics program for SPHERES satellites
- Student Space Programs Laboratory (Spring 2011 – Fall 2012)
  - Modeled power absorption of solar cells and researched effects of outer space environment on lithium-polymer batteries

Professional Presentations

- AIAA Region I-MA Student Conference, University of Maryland, MD
  - April 5-6, 2013
  - Presentation on "Numerical Modeling of a 17.8-GHz Microwave Electrothermal Thruster"